MOEM

Modern Electronic Materials 4(2): 71–75
DOI 10.3897/j.moem.4.2.38545

Research Article

# $CaSnO_3$: $Yb^{3+}$, $Er^{3+}$, $Ho^{3+}$ system synthesis and study of its luminescence under IR excitation

Ul'ana A. Mar'ina[1], Viktor A. Vorob'ev[1], Alexandr P. Mar'in[1]

*1 North-Caucasus Federal University, 1 Pushkina Str., Stavropol 355009, Russia*

Corresponding author: *Ul'ana A. Mar'ina* (ulyana-ne@mail.ru)

**Received** 13 July 2017 ♦ **Accepted** 10 May 2018 ♦ **Published** 1 June 2018

**Citation:** Mar'ina UA, Vorob'ev VA, Mar'in AP (2018) $CaSnO_3$: $Yb^{3+}$, $Er^{3+}$, $Ho^{3+}$ system synthesis and study of its luminescence under IR excitation. Modern Electronic Materials 4(2): 71–75. https://doi.org/10.3897/j.moem.4.2.38545

## Abstract

Solid state synthesis of Perovskite-like calcium stannate structure activated with three rare-Earth metal ions $Yb^{3+}$,$Er^{3+}$,$Ho^{3+}$ has been studied. The formation of the $CaSnO_3$ : $Yb^{3+}$,$Er^{3+}$,$Ho^{3+}$ luminescent structure requires the following synthesis conditions: anneal temperature 1250 °C and duration at least 18 h. The luminescent properties of the specimens have been studied under 960 nm semiconductor diode laser excitation. The luminescence spectra contain bands in the visible and IR spectral regions. $Yb^{3+}$ ions have been shown to act predominantly as sensibilizers capable of transferring part of absorbed energy to $Er^{3+}$ and $Ho^{3+}$ ions thus intensifying their respective luminescence peaks. $Er^{3+}$ ions also transfer part of absorbed energy to $Ho^{3+}$ ions leading to an increase in the intensity of the 1194 and 1950 nm IR luminescence bands. A schematic of possible energy transitions in the $CaSnO_3$ : $Yb^{3+}$,$Er^{3+}$,$Ho^{3+}$ system under 960 nm laser excitation has been suggested. The energy transfer mechanism between $Yb^{3+}$,$Er^{3+}$ and $Ho^{3+}$ions has been described in detail. The luminescence intensity of the luminophore has been studied at 994, 1194, 1550 and 1950 nm as a function of $Ho^{3+}$ion concentration. The peak intensity of the 1194 and 1950 nm bands is the highest at a $Ho^{3+}$ion concentration of 0.007 at.fr. It has been suggested to use the $CaSnO_3$ : $Yb^{3+}$,$Er^{3+}$,$Ho^{3+}$ luminescent structure for radiation sources capable of converting 960 nm IR radiation to ~2000 nm IR radiation.

## Keywords

luminescence, infrared luminophores, solid state synthesis, rare-Earth elements

## 1. Introduction

$CaSnO_3$ base compounds pertaining to $MSnO_3$ type Perovskite-like stannates find increasing application due to their universal electromagnetic properties. Currently they are of interest for multiple fields of electronics engineering as materials of cathodes, thermally stable capacitors, photocatalysts, gas or humidity sensors etc. [1, 2]. The luminescent properties of rare-Earth metal stannates have been studied insufficiently yet, most works dealing with calcium stannate compounds emitting visible radiation [3–6]. There are only a few works on IR luminescence of calcium stannate compounds in the 900–1600 nm region [7, 8]. No information on the luminescent properties of Perovskite-like stannates in the 1700–2000 nm region was available to us at the time we made this work. Therefore study of the luminescent properties of $CaSnO_3$ base compounds in this spectral region is an important research task.

Earlier experimental data for $CaSnO_3$ : $Yb^{3+}$, $CaSnO_3$ : $Er^{3+}$ and $CaSnO_3$ : $Ho^{3+}$ single-activator luminescent structures and double-activator $CaSnO_3$ : $Yb^{3+}$,$Er^{3+}$ and $CaSnO_3$ : $Yb^{3+}$,$Ho^{3+}$ luminescent structures indicated energy transfer from $Yb^{3+}$ ions to $Er^{3+}$ и $Ho^{3+}$ ones. This transfer increases the 1550 and 1950 nm luminescence band intensities, respectively. Below we consider the mechanism of energy transformation in the $Yb^{3+}$–$Er^{3+}$–$Ho^{3+}$ combination and the possibility of increasing IR luminescence intensity near 1950 nm by energy transfer to $Ho^{3+}$ ions from $Yb^{3+}$ and $Er^{3+}$ ones. To solve this task we synthesized series of specimens with the general formula $(Ca_{1-x-y-z}Yb_xEr_yHo_z)SnO_3$ and studied their luminescent properties.

## 2. Experimental

At the first stage we tested different solid state synthesis modes and selected optimum anneal temperature and time for pure $CaSnO_3$. The source components were calcium carbonate $CaCO_3$ and tin hydroxide $Sn(OH)_2$ which were dry mixed in the 1 : 1 stoichiometric ratio. After thorough grinding the charge was sieved (# 100 mesh), loaded into alundum crucibles and placed in a high-temperature furnace for heat treatment. The experiments showed that the formation of the pure $CaSnO_3$ phase requires specimen annealing in an oxidizing atmosphere at 1250 °C for 18 h [9].

At the second stage we obtained calcium stannate specimens activated with rare-Earth metal ions. The charge composition was calculated based on the formula $(Ca_{1-x-y-z}Yb_xEr_yHo_z)SnO_3$. The *x*, *y* and *z* indices in the formula correspond to the content of each element in the luminophore in atomic fractions. Since the luminescent properties of the test structures are sensitive to impurities the $CaSnO_3$ : $Yb^{3+}$,$Er^{3+}$,$Ho^{3+}$ system was synthesized from special purity $Yb_2O_3$, $Er_2O_3$ and $Ho_2O_3$ rare-Earth element oxides that were added to the charge in the form of nitrate solutions. The $Yb^{3+}$ ion concentration in the specimens was constant, 0.05 at.fr.. According to earlier data [10] this concentration provides for the highest 996 nm luminescence band intensity for the $(Ca_{0.95}Yb_{0.05})SnO_3$ system under 960 nm excitation. The $Er^{3+}$ ion concentration was 0.02 at.fr. and also constant. This concentration provides for the highest 1550 nm luminescence band intensity for the $(Ca_{0.93}Yb_{0.05}Er_{0.02})SnO_3$ system under 960 nm optical laser excitation [11]. The $Ho^{3+}$ ion concentration varied from 0.00005 to 0.1 at.fr.. Calcium carbonate and rare-Earth element nitrate solutions were mixed in liquid state and then the specimens were placed into a drying chamber for 2 h. Then a tin hydroxide and flux mixture was added to the charge, and the mixture was thoroughly grinded and sieved. Then the charge was loaded into alundum crucibles and annealed at 1250 °C for 18 h. The $SnCl_2$ (3 wt.%), $Li_2CO_3$ (1 wt.%) and $Na_2CO_3$ (1 wt.%) fluxes were added to the luminophore charge for reducing the melting point and increasing the solution component diffusion rate. Furthermore $Li^+$ and $Na^+$ alkaline metal ions act as compensating impurities. They partially compensate the charge mismatch produced by $Ca^{2+}$ ion substitution for $Yb^{3+}$, $Er^{3+}$ and $Ho^{3+}$ ions in $CaSnO_3$ lattice sites [5, 12, 13].

The phase composition of the as-synthesized specimens was studied on a DIFRAY-401 X-ray diffractometer ($CuK_\alpha$ radiation, Ni filter). The unit cell parameters were calculated using the Difract software. The grain size distribution of the powders was studied using a Microsizer-201A laser particle size analyzer. The luminescence and excitation spectra were taken in the 400–2100 nm range using an MDR-41 monochromator, FEU-62 and FEU-100 photoelectron amplifiers and a 960 nm pulse semiconductor diode laser.

## 3. Results and discussion

Calcium stannate $CaSnO_3$ has a perovskite-like orthorhombic crystalline structure with the *Pbnm* space symmetry group. Calcium stannate doping with rare-Earth element ions when $Yb^{3+}$, $Er^{3+}$ and $Ho^{3+}$ ions substitute $Ca^{2+}$ rare-Earth metal ions does not change the crystal lattice symmetry [14–16]. Figure 1 shows X-ray phase analysis data for the pure calcium stannate specimens synthesized at a constant temperature and different anneal times and for rare-Earth ion activated calcium stannate.

The position and intensity of the diffraction peaks correspond to the $CaSnO_3$ phase. The sharp diffraction peaks indicate the high crystallinity of the specimens. Grain size distribution analysis shows the average particle size of the $(Ca_{0.93-x}Yb_{0.05}Er_{0.02}Ho_{0.007})SnO_3$ structure to be 30.5 μm.

$(Ca_{0.93-x}Yb_{0.05}Er_{0.02}Ho_z)SnO_3$ structure excitation with 960 nm visible laser radiation produces anti-Stokes luminescence in the 540–560 nm and 640–690 nm bands (Fig. 2).

The 540–560 nm band does not show any clear holmium ion concentration dependence of luminescence intensity since this spectrum region is a superposition of luminescence peaks for multiple activators. The 545 nm peak for a 0.007 at.fr. $Ho^{3+}$ ion concentration is produced

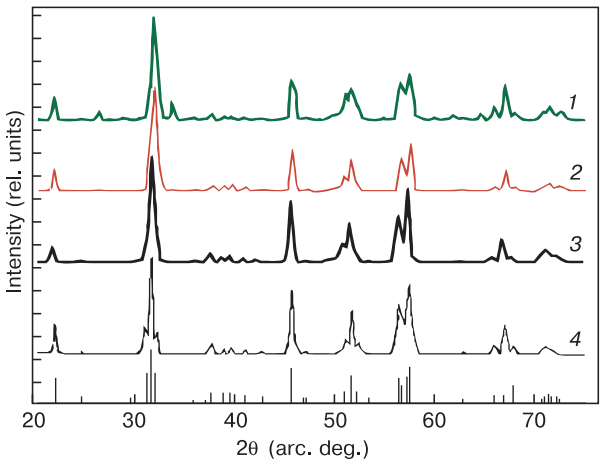


**Figure 1.** Diffraction patterns of $CaSnO_3$ specimens synthesized with (*1*) 1, (*2*) 10 and (*3*) 18 h anneal time and (*4*) $CaSnO_3$ : $Yb^{3+}$,$Er^{3+}$,$Ho^{3+}$ specimen synthesized for 18 h. The synthesis temperature was 1250 °C for all specimens.

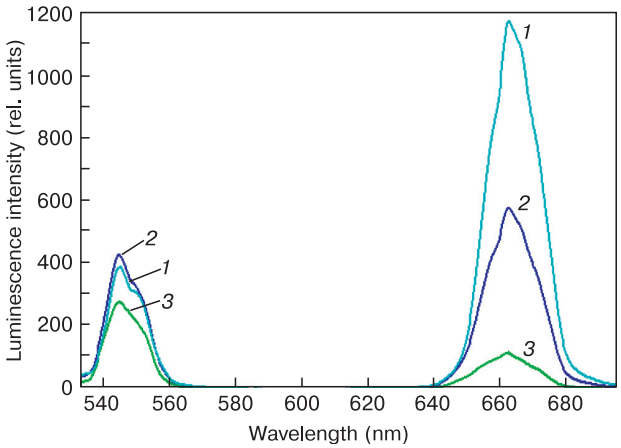


**Figure 2.** Visible luminescence spectra of $(Ca_{0.93-x}Yb_{0.05}Er_{0.02}Ho_z)SnO_3$ specimens ($z$ = 0.00005; 0.0005; 0.007) for 960 nm laser excitation: $z$ = (*1*) 0.00005 at.fr.; (*2*) 0.0005 at.fr.; (*3*) 0.007 at.fr.

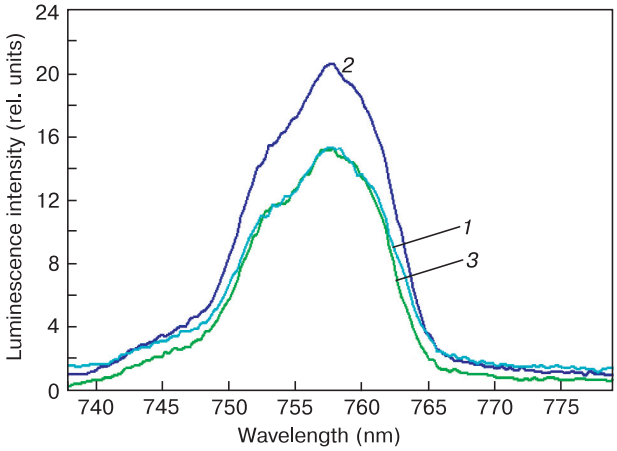


**Figure 3.** 740–775 nm luminescence spectra of $(Ca_{0.93-x}Yb_{0.05}Er_{0.02}Ho_z)SnO_3$ specimens for 960 nm laser excitation: $z$ = (*1*) 0.00005 at.fr.; (*2*) 0.0005 at.fr.; (*3*) 0.007 at.fr.

by the $^5F_4 \rightarrow {}^5I_8$ transition in holmium ions. The two other peaks in this band for 0.0005 and 0.00005 at.fr. holmium ion concentrations are at 545 and 550 nm and produced by the $^5F_4 \rightarrow {}^5I_8$ transition in holmium ions and the $^4S_{3/2} \rightarrow {}^4I_{15/2}$ transition in erbium ions, respectively. The luminescence intensity in the 640–690 nm band decreases with increasing $Ho^{3+}$ ion concentration in the luminophore. The luminescent peaks in this region are produced by the $^4F_{9/2} \rightarrow {}^4I_{15/2}$ transition in $Er^{3+}$ ions. Similar anti-Stokes luminescence was observed in the visible spectral region earlier [8, 13].

Weak luminescence was observed in the ~740–770 nm near IR region. This luminescence is produced by the $^5I_4 \rightarrow {}^5I_8$ transition in $Ho^{3+}$ ions (Fig. 3).

As the $Ho^{3+}$ ion concentration increases to 0.00005 at.fr. the luminescence intensity in this band increases and then decreases due to the concentration quenching of luminescence.

960 nm excitation of the material also produces IR luminescence bands peaking at ~996, 1194, 1550 and 1950 nm (Fig. 4).

The radiation in these bands corresponds to the following transitions:

- 996 nm band: $^2F_{5/2} \rightarrow {}^2F_{7/2}$ transition in $Yb^{3+}$ ions;
- 1194 nm band: $^5I_6 \rightarrow {}^5I_8$ transition in $Ho^{3+}$ ions;
- 1550 nm band: $^4I_{13/2} \rightarrow {}^4I_{15/2}$ transition in $Er^{3+}$ ions;
- 1950 nm band: $^5I_7 \rightarrow {}^5I_8$ transition in $Ho^{3+}$ ions.

Figure 3 shows that an increase in the $Ho^{3+}$ ion concentration in the luminophore matrix increases the luminescence intensity in the bands corresponding to $Ho^{3+}$ ions. However the bands corresponding to $Yb^{3+}$ and $Er^{3+}$ ions exhibit the contrary behavior. Earlier we reported that 811–960 nm laser excitation of specimens having a $(Ca_{1-x}Ho_x)SnO_3$ structure produces no luminescence but generates luminescence in the ($Yb^{3+}$, $Ho^{3+}$) and ($Er^{3+}$, $Ho^{3+}$) bands for the $(Ca_{1-x-y}Yb_xHo_y)SnO_3$ and $(Ca_{1-x-y}Er_xHo_y)SnO_3$ systems, respectively [10, 11]. Based on these data we concluded that these double-activator systems are activated through $Yb^{3+}/Er^{3+}$ ions acting as excitation centers. Part of energy is transferred from excited energy levels

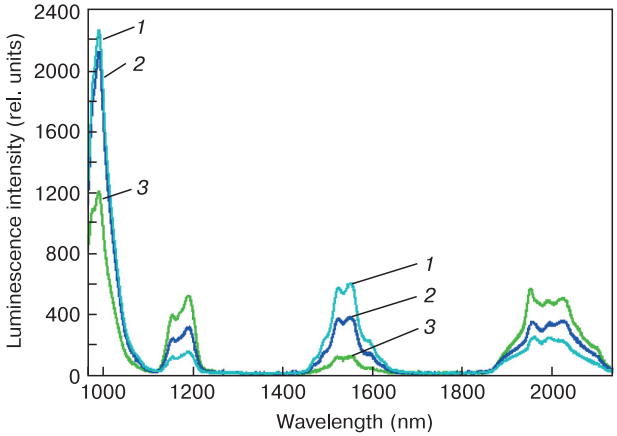


**Figure 4.** 1000–2150 nm luminescence spectra of $(Ca_{0.93-x}Yb_{0.05}Er_{0.02}Ho_z)SnO_3$ specimens for 960 nm laser excitation: $z$ = (*1*) 0.00005 at.fr.; (*2*) 0.0005 at.fr.; (*3*) 0.007 at.fr.

of $Yb^{3+}/Er^{3+}$ ions to $Ho^{3+}$ ion levels followed by optical transitions in $Ho^{3+}$ ions. The weak luminescence intensity of the $(Ca_{1-x-y}Er_xHo_y)SnO_3$ specimens compared with the $(Ca_{1-x-y}Yb_xHo_y)SnO_3$ ones indicates that $Yb^{3+}$ ions are more efficient sensibilizers than $Er^{3+}$ ones under IR excitation.

The luminescence peak intensity redistribution (Fig. 4) also indicates energy transfer from $Yb^{3+}$ and $Er^{3+}$ ions to $Ho^{3+}$ ones in the $(Ca_{0.93-x}Yb_{0.05}Er_{0.02}Ho_z)SnO_3$ luminescent system. The energy transformation mechanism in the $(Ca_{1-x-y-z}Yb_xEr_yHo_z)SnO_3$ triple-activator system can be described as follows.

1. Luminescent system excitation with a 960 nm source supplies sufficient energy for the core level electrons in $Yb^{3+}$ ($^2F_{7/2}$) and $Er^{3+}$ ($^4I_{15/2}$) ions to transit to the $^2F_{5/2}$ and $^4I_{11/2}$ excited states, respectively.
2. The energy absorbed by $Yb^{3+}$ ions is spent for phonon energy, the $^2F_{5/2} \rightarrow {}^2F_{7/2}$ radiative transition, energy transfer from the $^2F_{5/2}$ excited state of $Yb^{3+}$ ions to top energy levels of $Ho^{3+}$ and $Er^{3+}$ ions (cooperative sensibilization) and resonance interaction between $Yb^{3+}$ ($^2F_{5/2}$), $Ho^{3+}$ ($^5I_6$) and $Er^{3+}$ ($^4I_{11/2}$) ions.

3. $Yb^{3+}$–$Ho^{3+}$ ion pairs exhibit the following energy transformation processes: electron transition from the $^2F_{5/2}$ excited level of $Yb^{3+}$ ions to the $^3K_8$, $^5F_2$, $^5F_3$, $^5S_2$ and $^5F_4$ excited levels of $Ho^{3+}$ ions followed by anti-Stokes luminescence, and resonance energy transfer from the $^2F_{5/2}$ excited level of $Yb^{3+}$ ions to the $^5I_6$ excited level of $Ho^{3+}$ ions followed by Stokes IR luminescence.
4. $Yb^{3+}$–$Er^{3+}$ ion pairs exhibit the following energy transformation processes: electron transition from the $^2F_{5/2}$ excited level of $Yb^{3+}$ ions to the $^4F_{7/2}$ excited level of $Er^{3+}$ ions followed by anti-Stokes luminescence, and resonance energy transfer from the $^2F_{5/2}$ excited level of $Yb^{3+}$ ions to the $^4I_{11/2}$ excited level of $Er^{3+}$ ions followed by Stokes IR luminescence in the 1550 nm band.
5. $Er^{3+}$–$Ho^{3+}$ ion pairs exhibit the following energy transformation processes: resonance energy transfer from the $^4I_{11/2}$ excited level of $Er^{3+}$ ions to the $^5I_6$ excited level of $Ho^{3+}$ ions followed by Stokes IR luminescence.

The diagram of the abovementioned energy transitions in the visible and IR regions is presented in Fig. 5. The diagram was plotted using earlier data on the electron state energies of $Yb^{3+}$, $Er^{3+}$ and $Ho^{3+}$ ions [8, 17].

To specify more exactly the luminescence intensity in the 994, 1194, 1550 and 1950 nm bands as a function of $Ho^{3+}$ ion concentration we synthesized an additional series of specimens with $z$ = 0.001, 0.007, 0.01, 0.05 and 0.1 at.fr. (Fig. 6).

The luminescence intensity in the bands corresponding to ytterbium (994 nm) and erbium (1550 nm) ions is the highest at low $Ho^{3+}$ concentrations and decreases gradually with an increase in the holmium concentration. On the contrary, the luminescence intensity in the 1194 and 1950 bands corresponding to radiative transitions in

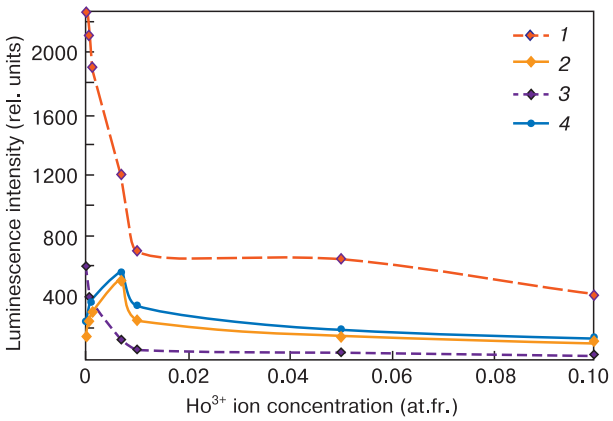


**Figure 6.** $(Ca_{0.93-x}Yb_{0.05}Er_{0.02}Ho_z)SnO_3$ luminescence intensity as a function of $Ho^{3+}$ concentration for (*1*) 994, (*2*) 1194, (*3*) 1550 and (*4*) 1950 bands.

holmium ions increases and peaks at $z$ = 0.007. Further increase in the holmium ion concentration in the luminophore matrix crystalline lattice intensifies concentration quenching of luminescence.

We used the best $(Ca_{0.943}Yb_{0.05}Ho_{0.007})SnO_3$ double-activator composition as a reference specimen for assessing the radiation efficiency of the $(Ca_{0.93-x}Yb_{0.05}Er_{0.02}Ho_z)SnO_3$ system in the ~2000 nm band when measuring the luminescence spectra for the specimens of this series. The study showed that the $(Ca_{0.923}Yb_{0.05}Er_{0.02}Ho_{0.007})SnO_3$ triple-activator composition has a higher luminescence intensity than the $(Ca_{0.943}Yb_{0.05}Ho_{0.007})SnO_3$ reference specimen at a 0.007 at.fr. $Ho^{3+}$ ion concentration. If the $(Ca_{0.943}Yb_{0.05}Ho_{0.007})SnO_3$ reference specimen intensity in the 1950 nm band is taken as 100%, the $(Ca_{0.923}Yb_{0.05}Er_{0.02}Ho_{0.007})SnO_3$ triple-activator composition specimen intensity is 25% higher in this band. This accounts for the experimentally observed increase in the holmium ion luminescence intensity in the ~2000 nm band.

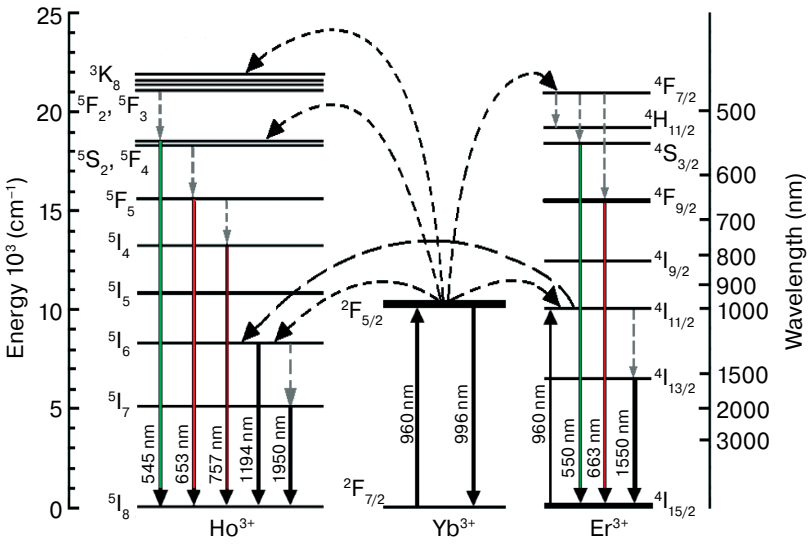


**Figure 5.** Schematic diagram of energy transfer mechanism between $Yb^{3+}$, $Er^{3+}$ and $Ho^{3+}$ ions in the $(Ca_{1-x-y-z}Yb_xEr_yHo_z)SnO_3$ system.

## 4. Summary

The interaction mechanism between $Yb^{3+}$,$Er^{3+}$ and $Ho^{3+}$ ions in the calcium stannate crystal lattice was described. The possibility of increasing IR radiation luminescence intensity in the 1950 nm region by energy transfer from $Yb^{3+}$ and $Er^{3+}$ ions to $Ho^{3+}$ ones was experimentally confirmed. The energy transfer mechanism and the radiative transition probability are largely controlled by the $Ho^{3+}$ ion concentration in the luminescent composition. The highest luminescence intensity in the 1950 nm band corresponds to a 0.007 et.fr. $Ho^{3+}$ ion concentration. The capability of the $CaSnO_3$ : $Yb^{3+}$,$Er^{3+}$,$Ho^{3+}$ luminescent system of converting near IR region radiation (960 nm) to greater wavelength radiation (~2000 nm) can be used for the fabrication of photoconverters, protective marks and markers and IR sources. 1500+ nm sources are widely used for information transmission via fiber optics communication lines and find increasing application in ophthalmology, detection/ranging and materials processing due to the eye-safety of this spectral region.

## References


1. Gavrilova L. Ya. *Metody sinteza i issledovanie perspektivnykh materialov* [Methods of synthesis and research of perspective materials]. Ekaterinburg: Ural State University named after A. M. Gorky, 2008, 74 p. (In Russ.)
2. Li H., Castelli I. E., Thygesen Kr. S., Jacobsen K. W. Strain sensitivity of band gaps of Sn-containing semiconductors. *Phys. Rev. B.* 2015; 91(4): 045204 (1–6). https://doi.org/10.1103/PhysRevB.91.045204
3. Bingfu Lei, Bin Li, Haoran Zhanga Wenlian Li. Preparation and luminescence properties of $CaSnO_3$:$Sm^{3+}$ phosphor emitting in the reddish orange region. *Optical Materials*. 2007; 29(11): 1491–1494. https://doi.org/10.1016/j.optmat.2006.07.011
4. Zhengwei Liu, Yingliang Liu. Synthesis and luminescent properties of a new green afterglow phosphor $CaSnO_3$ : Tb. *Mater. Chem. Phys.* 2005; 93(1): 129–132. https://doi.org/10.1016/j.matchemphys.2005.02.032
5. Zuoqiu Liang, Jinsu Zhang, Jiashi Sun, Xiangping Li, Lihong Cheng, Haiyang Zhong, Shaobo Fu, Yue Tian, Baojiu Chen. Enhancement of green long lasting phosphorescence in $CaSnO_3$ : $Tb^{3+}$ by addition of alkali ions. *Physica B: Condensed Matter.* 2013; 412: 36–40. https://doi.org/10.1016/j.physb.2012.12.013
6. Jinsu Zhang, Baojiu Chen, Zuoqiu Liang, Xiangping Li, Jiashi Sun, Lihong Cheng, Haiyang Zhong. Optical transition and thermal quenching mechanism in $CaSnO_3$ : $Eu^{3+}$ phosphors. *J. Alloys and Comp.* 2014; 612: 204–209. https://doi.org/10.1016/j.jallcom.2014.05.188
7. Orsi Gordo V., Tuncer Arslanli Y., Canimoglu A., Ayvacikli M., Galvro Gobato Y., Henini M., Can N. Visible to infrared low temperature luminescence of $Er^{3+}$, $Nd^{3+}$ and $Sm^{3+}$ in $CaSnO_3$ phosphors. *Appl. Radiation and Isotopes*. 2015; 99: 69–76. https://doi.org/10.1016/j.apradiso.2015.02.019
8. Pang X. L., Jia C. H., Li G. Q., Zhang W. F. Bright white upconversion luminescence from $Er^{3+}$–$Tm^{3+}$–$Yb^{3+}$ doped $CaSnO_3$ powders. *Optical Mat.* 2011; 34(1): 234–238. https://doi.org/10.1016/j.optmat.2011.08.019
9. Mar'ina U. A., Vorob'ev V. A. Features of synthesis the perovskitopodobnykh of structures like $MSnO_3$ ($M$ = Ba, Sr, Ca) and research of their luminescent properties. *Vestnik SKFU*. 2016; (1): 7–13. (In Russ.)
10. Mar'ina U. A., Vorob'ev V. A. The study of fluorescent properties of calcium stannate $CaSnO_3$, activated with rare earth metals. *Vestnik SKFU*. 2016; (4): 36–41. (In Russ.)
11. Mar'ina U. A., Mar'in A. P., Vorob'ev V. A. Synthesis and study of luminescent properties of system $CaSnO_3$ : $Yb^{3+}$,$RE^{3+}$ ($RE$ = Er, Ho,Tm). *Vestnik SKFU*. 2017; (2): 21–26. (In Russ.)
12. Mar'ina U. A., Vorob'ev V. A., Mar'in A. P. Vliyanie kontsentratsii primesi Yb i tipa plavnya na lyuminestsentnye svoistva $CaSnO_3$ : Yb [Influence of concentration of Yb impurity and type of mineralizer on luminescent properties $CaSnO_3$ : Yb]. Nauchnye issledovaniya i razrabotki molodykh uchenykh: materialy XIV mezhdunar. molodezhnoi nauchno-prakt. konf = *Research and development of young scientists: materials XIV of the international youth scientific and practical conference*. Novosibirsk: Publishing House TsRNS, 2016. (In Russ.)
13. Tao Pang, Wenhui Lu, Wujian Shen. Chromaticity modulation of upconversion luminescence in $CaSnO_3$ : $Yb^{3+}$, $Er^{3+}$, $Li^{+}$ phosphors through $Yb^{3+}$ concentration, pumping power and temperature. *Physica B: Condensed Matter.* 2016; 502: 11–15. https://doi.org/10.1016/j.physb.2016.08.036
14. Castelli I. E., Olsen T., Datta S., Landis D. D., Dahl S., Thygesen Kr. S., Jacobsen K. W. Computational screening of perovskite metal oxides for optimal solar light capture. *Energy Environ. Sci.* 2012; 5(2): 5814–5819. https://doi.org/10.1039/C1EE02717D
15. Henriques J. M., Caetano E. W. S., Freire V. N., da Costa J. A. P., Albuquerque E. L. Structural, electronic, and optical absorption properties of orthorhombic $CaSnO_3$ through *ab initio* calculations. *J. Physics: Condensed Matter.* 2007; 19(10): 106214 (1–9). https://doi.org/10.1088/0953-8984/19/10/106214
16. Protasov N. M. *Strukturnoe modelirovanie slozhnykh oksidov so strukturoi perovskita v chastichno kovalentnom priblizhenii* [Structural modeling of complex oxides with structure of a perovskite in partially covalent approach]. Moscow: MGU im. M. V. Lomonosova, 2011, 51 p. (In Russ.)
17. Savikin A. P., Grishin I. A. *Sintez keramicheskikh obraztsov ZBLAN : $Ho^{3+}$ i ZBLAN : $Ho^{3+}$–$Yb^{3+}$ i issledovanie antistoksovoi lyuminestsentsii* [Synthesis of ceramic samples of ZBLAN : $Ho^{3+}$ both ZBLAN : $Ho^{3+}$–$Yb^{3+}$ and research of an anti-Stokes luminescence: educational and methodical grant]. Nizhny Novgorod: Nats. issled. NGU im. N. I. Lobachevskogo, 2016, 18 p. (In Russ.)
18. Solid-state lasers with semiconductor pump of short- and average IR-ranges (2 micron, 3–8 micron) on the basis of crystals and ceramics, activated by ions Tm и Ho. Report on research work, head Ryabochkina P. A.; performers: Antipov O. L., Chuprunov E. V., Lomonova E. E. Saransk, 2012, 83 p. (In Russ.)
19. Bailey D., Wright E. *Volokonnaya optika: teoriya i praktika* [Practical fiber optics]. Moscow: KUDITs-PRESS, 2008, p. 98. (In Russ.)
20. Shakhno E. A. *Fizicheskie osnovy primeneniya lazerov v meditsine* [Physical bases of use of lasers in medicine]. St. Petersburg: NIU ITMO, 2012, 129 p. (In Russ.)